Geomechanics and Engineering, *Vol. 26, No. 2 (2021) 147-160*
https://doi.org/10.12989/gae.2021.26.2.147

Establishing an opening size criterion in direct shear test using DEM Simulation

Byeong-Su Kim*

Graduate School of Environmental and Life Science, Okayama University,
3-1-1 Tsushima-naka, Kita-ku, Okayama City, Okayama 700-8530, Japan

(Received February 15, 2021, Revised June 5, 2021, Accepted June 29, 2021)

Abstract. Direct shear test has been widely used to examine the shear strength of geomaterials because of the simplicity of the testing method and apparatus. Three factors significantly affect the accuracy of the experimental results of direct shear tests, namely (1) the type of direct shear apparatus, (2) the specimen size (scale effect), and (3) the opening size between shear boxes. This study focused on the Threshold Line (TL), which is obtained based on experimental tests, as a guideline for setting the opening size between the shear boxes. The validity of the TL was examined using distinct element method (DEM) 3D simulations from the following four perspectives: the first and second perspectives investigated the influence of the mean particle size and particle size distribution for mean particle sizes larger than 0.8 mm. In the third perspective, the scale effect of the specimens for fixed and varying D:H ratios of the shear box to reduce the shear box size was examined. Lastly, in the fourth perspective, the validity of using the TL to determine the appropriate opening size for the samples with a mean particle size smaller than 0.8 mm was also examined based on the Threshold Point (TP). For each case, the results of the TPs obtained from the DEM simulations agreed well with those of the TL. These findings suggest that the TL is valid and the TL relational equation can be used for setting the opening size between the shear boxes in the direct shear test regardless of saturated and unsaturated soils.

Keywords: DEM simulation; direct shear test; opening size; threshold line (TL); threshold point (TP)

1. Introduction

Ground disasters such as slope failure, landslides, and liquefaction caused by rainfall or earthquakes have resulted in the destruction of infrastructure and the loss of lives and property. To prevent these damages, studies have measured and evaluated the shear strength characteristics of the ground with infiltration, such as the cohesion and the internal friction angle (ϕ) (Ng and Shi 1998, Wang 2003, Cho 2008, Kim *et al*. 2010, Oh and Vanapalli 2018, Lin *et al*. 2018). The laboratory testing methods that are generally used for this purpose in the field of geotechnical engineering are triaxial compression tests, unconfined compression tests, and direct shear tests. In particular, the direct shear test has been widely used to examine the shear strength properties of geomaterials because of the simplicity of its testing method and apparatus (e.g., Scarpelli and Wood 1982, Jewell and Wroth 1987, Gan *et al*. 1988, Palmeira and Milligan 1989, Shibuya *et al*. 1997, Vanapalli *et al*. 1996, Hight and Leroueil 2003, Cerato and Lutenegger 2006, Guo 2008, Kim *et al*. 2010, 2012, 2013, Caruso and Tarantino 2015; Lee *et al*. 2017; Sweta and Hussaini 2018, Meguid and Khan 2019). Unfortunately, direct shear tests have the potential to yield different results even if the same sample is tested under the same conditions. This tendency could be mainly caused by three factors, namely (1) the type of direct shear apparatus, (2) the specimen size (scale effect), and (3) the opening size (d) between the shear boxes (Shibuya *et al*. 1997, Kim *et al*. 2012). In particular, the opening (or gap) size between the shear boxes substantially affects the shear strength and deformation in direct shear tests. In the case of a direct shear test with no opening between the shear boxes, a concentrated compression zone appears around the shear plane, in which an exaggerated dilatancy and non-uniformity in the deformation of the specimen occur (Yatabe *et al*. 1995). Shibuya *et al*. (1997) reported that the larger the opening size up to 5.0 mm, the smaller the internal friction angle (ϕ) because of an outflow of the material through the opening. They also reported that the opening size should be larger than the size of the shear band in the specimen, and the minimum value of opening for the internal friction angle (ϕ) corresponded related closely to the thickness of the shear band observed in the plane strain compression tests by Tatsuoka *et al*. (1990). A suitable opening size should be applied to make the deformation mode of the simple shear for a specimen. Thus, the opening size between the shear boxes affects the reliability of direct shear tests.

According to ASTM 3080-04 (2009), the setting criterion for the opening or gap is expressed as follows: "There may be instances when the gap between the plates should be increased to accommodate sand sizes greater than the specified gap. Presently there is insufficient information available for specifying gap dimension based on particle

*Corresponding author, Associate Professor (Dr.Eng.)
E-mail: bskim@okayama-u.ac.jp

ISSN: 2005-307X (Print), 2092-6219 (Online)

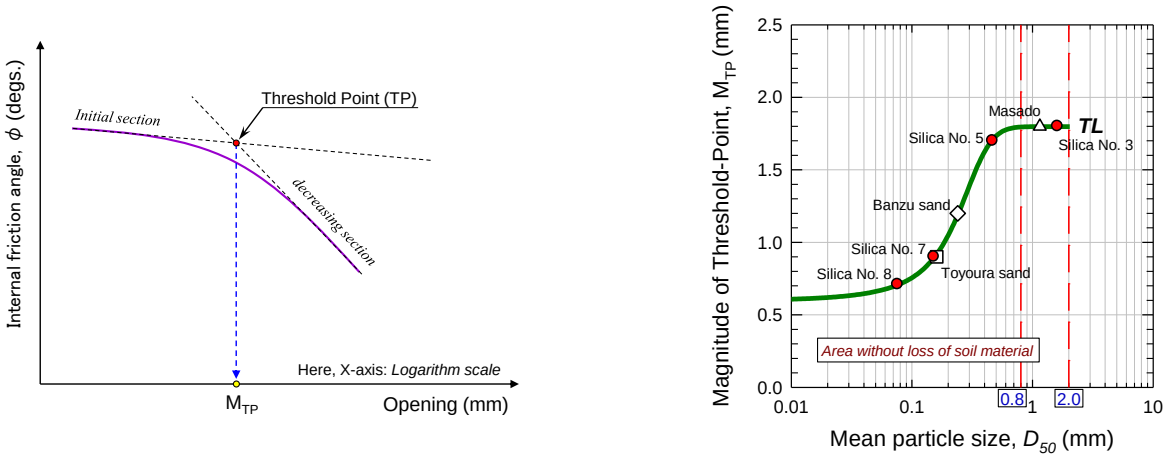

(a) Notion of Threshold-Point (TP) (b) Notion of Threshold-Line (TL)

Fig. 1 Notion of Threshold-Point (TP) and the Threshold-Line (TL) proposed as a guideline for setting the opening size between the shear boxes in the direct shear test (Modified after Kim *et al*. 2012)

Table 1 Physical properties of soil samples used in the study of Kim *et al.* (2012)

Soil samples	G_s	e_{max}	e_{min}	D_{50} (mm)	C_c	C_u
Toyoura sand	2.64	0.98	0.61	0.16	1.22	1.38
Masado	2.65	-	-	1.15	4.38	161.72
Banzu sand	2.73	1.09	0.65	0.24	0.91	2.64
Silica sand No.3	2.64	1.03	0.72	1.61	0.97	1.46
Silica sand No.5	2.64	1.03	0.68	0.47	1.18	1.38
Silica sand No.7	2.62	1.18	0.67	0.15	1.10	1.81
Silica sand No.8	2.62	1.41	0.72	0.08	-	-

Note: G_s: Specific gravity, e_{max}: maximum void ratio, e_{min}: Minimum void ratio, D_{50}: Mean particle size, C_c: Coefficient of curvature, C_u: Coefficient of uniformity

size distribution." The criterion for the opening size in the direct shear test is still ambiguous. However, few studies have been carried out to determine the appropriate opening size between shear boxes for various types of soil samples. Kim *et al*. (2012) studied the influence of the opening between the shear boxes (20 mm in height and 60 mm in diameter) on the shear behavior in direct shear tests under a constant pressure condition using seven types of granular material. The physical properties of soil samples used in the study of Kim *et al*. (2012) are summarized in Table 1. They reported that as the opening size increases, the magnitude of the shear strength and dilatancy decreases due to the outflow of the sample from the opening between shear boxes. They proposed the notion of the Threshold Point (TP) in terms of the relationship between the opening size and the internal friction angle (ϕ), as shown in Fig. 1(a). The TP was defined as the intersection point between the tangent of the initial section and the tangent of the decreasing section. That is, the TP can be understood as the opening size at which the internal friction angle (ϕ) decreases sharply with increasing opening size. It should be noted that the initial conditions of void ratio or dry density do not affect the magnitude of the Threshold Point (M_{TP}). Based on the obtained results, they defined the Threshold Line (TL) as a criterion for the opening size between shear boxes. The TL was defined based on all the TPs in the relationship between the internal friction angle (ϕ) and the mean particle size (D_{50}), as shown in Fig. 1(b). If the opening size is set based on the TL in the direct shear test, it is possible to obtain a reasonable internal friction angle (ϕ) without the influence of the sample outflow during shearing. In particular, in the study of Kim *et al*. (2012), the specimen of 'Masado' was tested under the saturated condition, while the other samples were tested under the unsaturated condition. It can be understood that the outflow from the opening between the shear boxes is related to only the particle size. Therefore, it is expected that the TL could provide a guideline for determining an adequate opening size in direct shear tests regardless of saturated and unsaturated soils.

In this study, to verify the validity of the TL as a guideline for selecting the opening size between the shear boxes, the influence of the mean particle size (D_{50}) and particle size distribution on the TL was examined for various granular materials using a distinct element method (DEM) 3D simulation. This study was divided into four parts. In the first and second parts, the simulations were conducted to investigate the influence of the mean particle size (D_{50}) and particle size distribution for mean particle sizes larger than 0.8 mm on the TL. In the third part, the scale effect of the specimens was examined for fixed and varying D:H ratios of the shear box for a mean particle size

smaller than 0.8 mm. The scale effect of specimens in the direct shear test for a mean particle size smaller than 0.8 mm was verified through DEM simulation, and it was determined whether the shear box size could be adjusted. Lastly, in the fourth part, the validity of the TL to determine the appropriate opening size for the samples with a mean particle size smaller than 0.8 mm was verified based on the results of the TP obtained from the DEM 3D simulations.

2. DEM simulation of direct shear test

2.1 Contact model

Since the DEM was proposed by Cundall (1971) and Cundall and Strack (1979) as a numerical approach to solve the action of the discrete element models for granular materials, many studies of direct shear tests using DEM simulations have been performed (e.g., Thornton 2000, Ni *et al.* 2000, Liu 2006, Zhang and Thornton 2007, Yan 2009, Kim *et al.* 2014, Xu *et al.* 2015, Suhr *et al.* 2018, Bian *et al.* 2019, Kodicherla *et al.* 2019). In this study, the DEM simulations of direct shear tests were performed using the three-dimensional PFC (Particle Flow Code) program (Itasca 2005). In the DEM simulation, it is important to determine suitable parameter values to obtain acceptable results. In order to determine suitable parameters, the contact model for an elastic column, or the Hertz-Mindlin theory, can be applied to determine the stiffness of elastic springs at contact points. Since glandular materials such as sand deform with rearrangement of the particles and the change of the void space between the particles, the spring stiffness can be applied, which reduces the amount of overlap between particles. In this study, the spring stiffness was determined using a linear model for the relative movement between particles based on simple dynamic models such as the Voigt model and Coulomb's friction rule. The motion of each particle arising from the contact and body forces was determined by Newton's second laws as follows:

$$F_i = m\left(\frac{\partial^2 x_i}{\partial t^2} - g_i\right) \ (i=1,2,3) \tag{1}$$

$$M_i = I\frac{\partial^2 \varphi_i}{\partial t^2} \quad (i=1,2,3) \tag{2}$$

where F_i= the resultant force, the sum of all externally applied forces acting on the particle; x_i= the contact location between the particles; g_i= the body force acceleration vector (e.g., gravity loading); m= a mass of the particle; I= the moment of inertia of the particle; M_i= the unbalanced moment for the particle; and φ_i= a rotation of the particle.

$$F^s_{\max} = \mu\left|F^n_i\right| \quad (i=1,2,3) \tag{3}$$

$$F^n_i = K^n \cdot U^n \cdot n_i \quad (i=1,2,3) \tag{4}$$

where μ= the friction coefficient, which is taken to be the minimum friction coefficient of the two contacting entities; F_i^n= the normal contact force vector; K^n= the normal stiffness at the contact; U^n= the relative normal displacement between two particles; and n_i= the unit normal vector. Note that the normal stiffness is a secant modulus related to the total displacement and force.

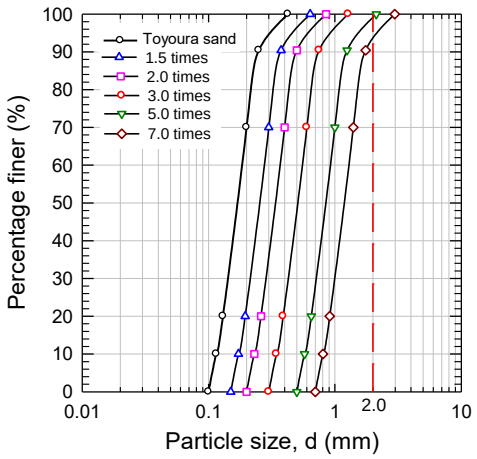

Fig. 2 The particle size distributions of samples defined on the basis of Toyoura sand

In the contact model, a particle of granular material is treated as an element of a rigid sphere. Each particle can be in contact with adjacent particles or boundaries (e.g., wall). The contact model consists of a pair of dashpots for normal and shear viscous dampings, and elastic springs with constant normal and shear stiffnesses acting at the contact point. The two elastic springs have specified shear and tensile normal strengths related to the contact bond. The existence of a contact bond precludes the possibility of slip (i.e., the magnitude of the shear contact force is not adjusted to the allowable maximum shear contact force, $F^s_{\max}$ of Eq. (3)). Instead, the magnitude of the shear contact force is limited by the shear contact bond strength. Contact bonds also allow tensile forces to develop at a contact. Thus, the contact forces induced by the relative movement of the particle depend on the contact model. The frictional resistance at the contact point depends on the slider for the shear direction. In the DEM simulation, since the slip condition between the particles is determined based on the allowable maximum shear contact force, the magnitude of the shear contact force is kept less than the allowable maximum shear contact force. As described above, the magnitude of the shear contact force is limited by the shear contact bond strength. The shear contact forces are caused by the application of the normal contact force vector (i.e., Eq. (4)) when there is no overlap between the particles, that is, the relative normal displacement (U^n) between two particles is negative.

The contact bond can be defined by the two parameters: normal contact bond force (F^n) and shear contact bond force (F^s). If the normal contact force (F^n) at the contact is greater than 0, tension occurs. Since the normal contact model in tension is defined by the normal stiffness at the contact, if there is no overlap, the particle is allowed to slide. However, if the shear contact bond force (F^s) does not exceed the friction limit and the normal contact bond force is in compression, the contact forces do not change. Whereas, if the magnitude of the shear contact force (F^s)

Table 2 Input parameters for particle and wall in the DEM simulation

Parameters	Values
Density of particles (kg/m^3)	2600
Normal stiffness of particles, k_n (N/m)	1.0×10^6
Shear stiffness of particles, k_s (N/m)	2.5×10^5
Normal stiffness of axial walls, k_n (N/m)	1.0×10^6
Normal stiffness of lateral walls, k_n (N/m)	1.0×10^9
Shear stiffness of walls, k_s (N/m)	0.0
Friction coefficient between particles	0.5
Friction coefficient between particle and wall	0.0
Local damping coefficient	0.7

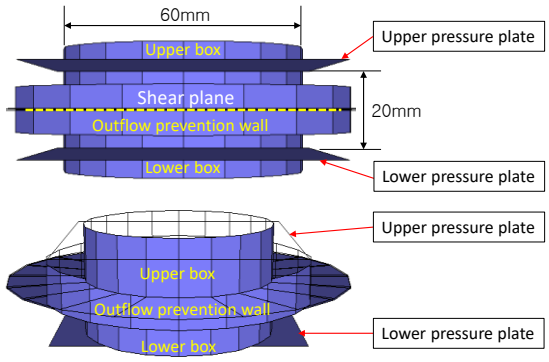

Fig. 3 Modeling of the shear box for the DEM simulation of the direct shear test

equals or exceeds the shear contact bond strength, the bond breaks (i.e., slip condition).

2.2 Characteristics of samples and parameters used in DEM Simulation

As shown in Fig. 2, the grain size distribution curves of the samples used in the DEM simulation were defined according to each case based on the grain size distribution curve of Toyoura sand in order to maximize the computational processing capability. Toyoura sand is a standard sand in the field of geotechnical engineering in Japan and has the following physical properties: a soil particle density (ρ_s) of 2.640 g/cm^3; a mean grain size of 0.161 mm; maximum and minimum void ratios of 0.977 and 0.605, respectively; a coefficient of curvature (C_c) of 1.22; and a coefficient of uniformity (C_u) of 1.38. Since the maximum particle diameter of the samples used to obtain the TL in the experiment of Kim *et al*. (2012) was 2.0 mm, in the present study, a maximum particle diameter of 2.0 mm was used in the simulation. In the case of the specimens smaller than standard size (i.e., 20 mm in height and 60 mm in diameter) described later, the minimum particle diameter was adjusted according to each simulation condition to properly control the number of balls generated for efficient DEM simulation. All specimens were generated with an initial void ratio (e) of 0.81. The generated specimens were under a loose condition state with a relative density (D_r) of 55.1%.

The input parameters for particles and walls in the DEM simulation are summarized in Table 2. The values of the shear spring stiffness for the normal and shear directions were obtained from Oda and Iwashita (2000). To reproduce the relationship between the actual shear box and the particle on the lateral interface, the value of the normal stiffness of the lateral wall was set to 1.0×10^9 N/m, the value of the shear stiffness of walls was set to 0.0 N/m, and the coefficient of friction between the particle and the wall was set to 0.0. In the direct shear test, since the volume of the specimen changes by the vertical movement of the upper loading plate, the value of the normal stiffness of the upper and lower walls in the DEM analysis was set to 1.0×10^6 N/m (i.e., different to that of the lateral wall). The friction coefficient between particles was set as 0.5 based on the physical friction coefficient of Toyoura sand. The local damping coefficient was generally set to 0.7 in the PFC-3D program (Itasca 2005).

2.3 Modelling of shear box in DEM simulation

In the DEM 3D simulation, a shear box of the same size as that used in the study of Kim *et al*. (2012) (diameter 60 mm, height 20 mm) was first assembled using wall elements. Fig. 3 shows the side view of the shear box reproduced in the DEM 3D simulation of the direct shear test. The shear box is composed of side walls (cylindrical type: 60 mm in diameter) and upper and lower pressure walls (plates). The upper pressure plate was installed 20 mm above the lower pressure plate so that the height of the specimen was 20 mm. The shear box is displayed as 20 columns in the PFC-3D program. During analysis, only the upper pressure plate (upper wall) moves up and down in response to the volume change of the specimen. Additionally, outflow prevention walls were installed on the shear plane between the upper and lower shear boxes in order to avoid dispersing balls (i.e., the soil particles) far away from the specimen when the balls were leaked through the opening between the shear boxes. These outflow prevention walls reduce the analysis time for the locations of the leaked balls in the DEM simulation. First, the upper and lower outflow prevention walls, whose diameter was twice that of the specimen were installed horizontally with respect to the upper and lower shear boxes, as shown in Fig. 3. Namely, the inner shape of the upper and lower outflow prevention walls is the same as a flat donut having an inner diameter of 60 mm and an outer diameter of 120 mm in a plan view. The installation location of the upper outflow prevention wall was changed according to the opening size between the shear boxes. To prevent the balls from scattering between the two outflow prevention walls, another outflow prevention wall with a cylindrical shape and a height of 10 mm was installed vertically with respect to the shear plane as show in Fig. 3.

2.4 Modelling of shear box in DEM simulation

After the modeling of the shear box for the DEM 3D simulation of the direct shear test was completed, the second step was the process of generating particles (balls) to reproduce the specimen. The particles were generated

inside the shear box in accordance with the particle size distributions defined for each case and with an initial void ratio of 0.81. The third step was the compression (consolidation) of the specimen. In the compression process, a vertical stress of 300 kPa was applied to the specimen by compression of the upper pressure plate, and the compression speed of the upper pressure plate was controlled. The criterion for the completion of the compression process was defined as the state when the stress of the load (pressure) plate was within an error of 0.5% of the target vertical stress (i.e., 300 kPa). The fourth step was to set the opening between the shear boxes before the shearing process. The opening was set by reducing the height of the upper shear box near the shear plane. For example, if the opening size was 0.2 mm, the height of the upper shear box becomes was reduced by the opening size (i.e., d= 0.2mm) before the shearing process.

Furthermore, in the shearing process, only the upper pressure plate was controlled to keep the predetermined vertical stress of 300 kPa on the specimen. Then, only the lower shear box involving the lower pressure plate and the lower outflow prevention wall moved horizontally at a constant shear rate. The specimen was sheared until the maximum shear strength was confirmed. The shearing process was performed while maintaining the opening size by fixing the shear box vertically, as in the real direct shear test. The shear stress on the specimen was calculated by dividing the unbalanced force in the shear direction on the side wall of the lower shear box by the cross-sectional area of the specimen. The horizontal and vertical displacements during shearing were determined based on the horizontal movement distance of the lower shear box, and the vertical movement distance of the upper pressure wall, respectively. Moreover, gravity was applied to examine the shear behavior under the same boundary stress conditions as in the real direct shear test.

3. Verification on the influence of particle size distribution and D_{50} on TL

3.1 Verification using samples with different particle size distributions and the same mean particle size

To examine the validity of the TL on the influence of particle size distribution (i.e., variation of contents of the contents of fine and coarse particles), DEM 3D simulations for Case 1 were performed using a sample with a fixed average particle size (D_{50}) and a particle size distribution seven times larger than that of Toyoura sand, as shown in Fig. 2. In Case 1, this grain size distribution curve was simplified into a straight line and was defined as a standard line of sample A1, as shown in Fig. 4. The particle size distribution curves with slopes that are 1/2, 1/3, and 1/4 times the slope of sample A1 with a mean grain size of 1.25 mm were defined as samples B, C, and D, respectively, in Case 1. The change in the inclination of the particle size distribution indicates that the ratios of the granular and fine particles of the sample change. The simulations for Case 1 were performed to verify the shear behavior for different contents of fine and coarse particles. Thus, the variation of

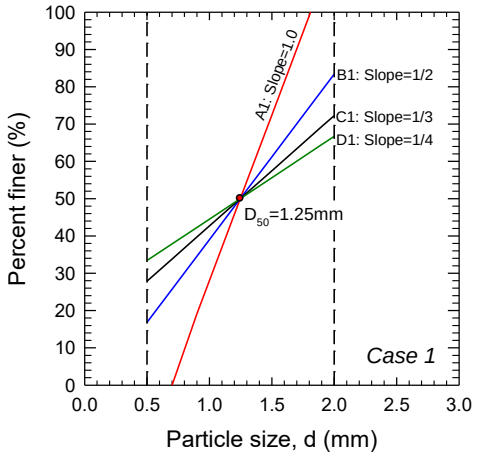

Fig. 4 Samples with changed particle size distribution based on sample A1 with particle size of 7 times for Toyoura sand in Case 1

Table 3 The simulation condition and the results of the MTP for Case 1

Samples	D_{50} (mm)	Passing percent for particle size		Particle number	M_{TP} (mm)
		0.5 mm	2.0 mm		
A1: slope=1.0	1.25	0.0	100.0	46,370	1.81
B1: slope=1/2		16.8	83.4	95,822	1.72
C1: slope=1/3		27.9	72.3	110,558	1.72
D1: slope=1/4		33.4	66.7	118,233	1.67

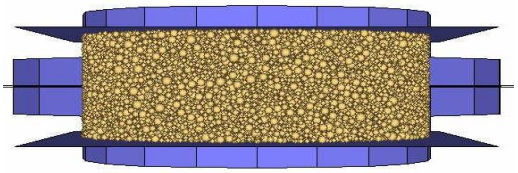

Fig. 5 Specimen of sample D1 (slope=1/4 and particle number: 118,233) reproduced in the DEM simulation

the magnitude of the TP could be observed on the four patterns of the particle size distribution curve.

In Case 1, the range of particle sizes was limited from 0.5 to 2.0 mm. The minimum value of 0.5 mm was chosen to prevent the excessive increase in the number of balls, and the maximum value of 2.0 mm was adopted because this was the maximum size of soil particles in the experimental direct shear test (e.g., Kim *et al*. 2012). The minimum and maximum particle diameters of each sample were, respectively, as follows: sample A1: 0.7 mm and 1.8 mm; and samples B1, C1, and D1: 0.5 mm and 2.0 mm. The simulation condition of each sample in Case 1 are summarized in Table 3.

As described above, the direct shear test in the DEM 3D simulation was conducted via the following three steps. The first step was the process of generating particles inside the shear box to reproduce the specimen. Four types of samples were generated for an initial void ratio of 0.81 inside the shear box, such as sample D1 in Fig. 5. The particle numbers of each sample were as follows: sample A1

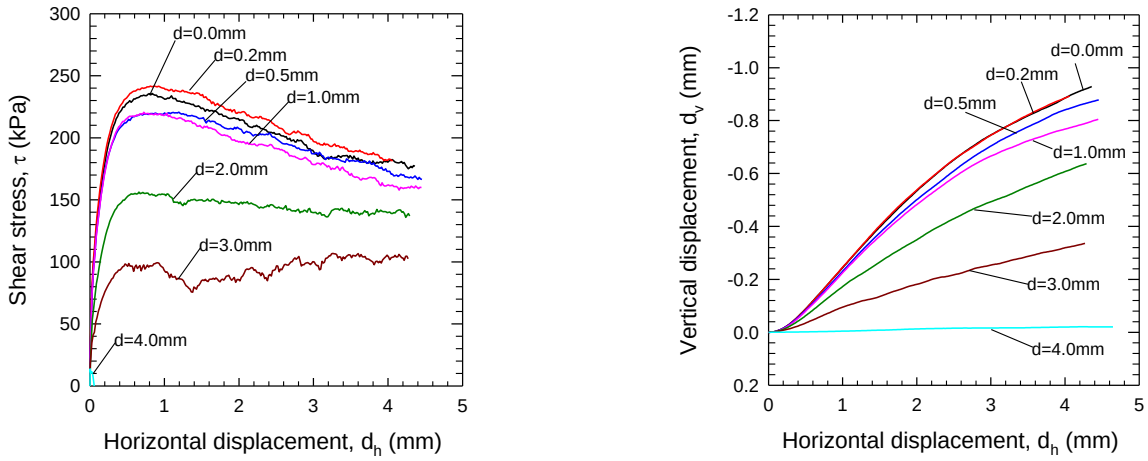

(a) d_h vs. τ (b) d_h vs. d_v

Fig. 6 Results of DEM simulation for sample A1 (slope=1.0, and particle number: 46,370)

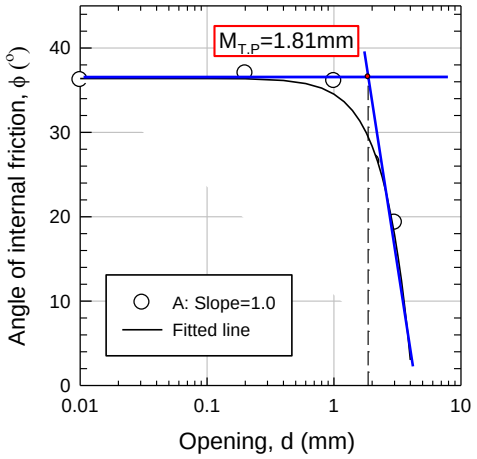

Fig. 7 Determination of the magnitude of Threshold-Point (TP) for sample A1 (slope=1.0, particle number: 46,370)

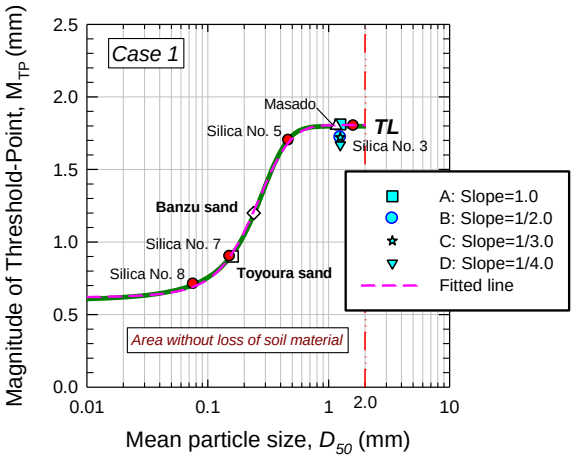

Fig. 8 Comparison of the results of the M_{TP} in Case 1 and the TL

(slope=1.0): 46,370; sample B1 (slope=1/2): 95,822; sample C1 (slope=1/3): 110,558; and sample D1 (slope=1/4): 118,233. The second step was the compression (consolidation) of the specimen. In the compression process, a vertical stress of 300 kPa was applied to each sample. Before the shearing process, opening sizes of 0.0, 0.2, 0.5, 1.0, 2.0, 3.0, and 4.0 mm were set by reducing the height of the wall near the shear plane of the upper shear box as in the study by Kim *et al*. (2012). Then, the shearing process was carried out under a vertical stress of 300 kPa.

Table 4 Results of the internal friction angle (ϕ) according to the opening size for Case 1

Opening size, d (mm)	Internal friction angle, ϕ (degs.)			
	A1	B1	C1	D1
0.0	36.2	37.2	37.6	36.1
0.2	37.0	36.9	35.3	35.9
0.5	34.8	36.0	37.0	35.5
1.0	36.1	33.7	33.6	35.0
2.0	26.5	28.4	27.2	25.2
3.0	19.3	9.5	8.7	8.5
4.0	-	-	-	-

Figs. 6(a) and 6(b) show the relationship between the horizontal displacement (d_h) and the shear stress (τ), and the relationship between the horizontal displacement (d_h) and the vertical displacement (d_v), for sample A1 (slope =1.0, particle number= 46,370). When comparing the relationships between horizontal displacement and shear stress for all opening sizes except for d= 4.0 mm (i.e., d=0.0, 0.2, 0.5, 1.0, 2.0, and 3.0 mm), the shear stress increases rapidly in the initial stage of shearing, and the maximum shear stress occurs at a horizontal displacement of around 1.0 mm. The shear stress decreases as the opening size increases. Meanwhile, when comparing the relationship between horizontal displacement and vertical displacement, the dilatancy increases as the horizontal displacement increases in all cases except for d= 4.0 mm. In particular, in the case of d= 3.0 mm, although the shear stress decreased after the maximum shear stress and then increased with the dilative behavior again. This tendency can be understood as the effect of the rearrangement of the particles in the shear plane during the shear process. Therefore, these results indicate that the larger the opening size, the smaller the

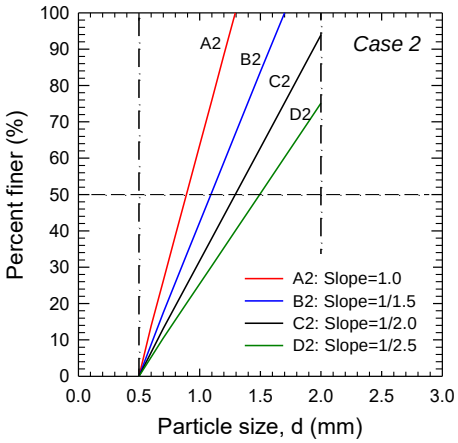

Fig. 9 Samples with changed particle size distribution based on sample A2 with particle size of 5 times for Toyoura sand

Table 5 Simulation condition and the results of the MTP for Case 2

Samples	D_{50} (mm)	U_c	Particle number	M_{TP} (mm)
A2: slope=1.0	0.89	1.69	129,233	1.87
B2: slope=1/1.5	1.08	1.98	86,269	1.97
C2: slope=1/2.0	1.28	2.23	68,962	1.87
D2: slope=1/2.5	1.49	2.46	56,756	1.77

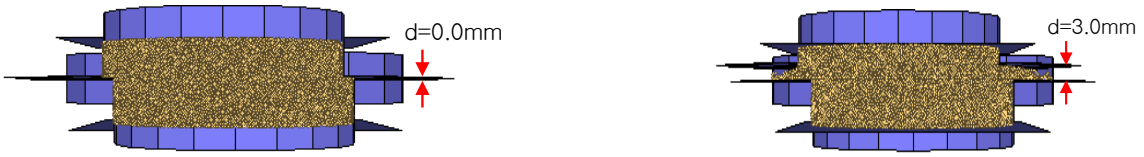

(a) d= 0.0 mm (b) d= 3.0 mm

Fig. 10 The state of the particles for specimens of sample A2 after the shearing process for opening sizes of d= 0.0 and d= 3.0 mm

dilatancy. For d= 4.0 mm for each sample, a large number of particles to flow out of the opening between the shear boxes were observed at the beginning of the shearing process, and it is therefore judged that the behaviors of the shear strength and the dilatancy were not manifested.

The shear stress in the DEM simulation was determined from the unbalanced force of the upper shear box. The results of the internal friction angle (ϕ) obtained from the maximum shear stress of each specimen for different opening sizes are summarized in Table 4. It can be observed that when the opening size increases beyond a certain size, the internal friction angle (ϕ) decreases rapidly. The M_{TP} (i.e., the magnitude of Threshold Point) for each sample was determined from the relationship between the opening size and the internal friction angle (ϕ) using the determination method of Kim *et al*. (2012), as shown in Fig. 7. The M_{TP} for samples A1, B1, C1, and D1 were 1.81, 1.72, 1.72, and 1.77 mm, respectively. Fig. 8 shows the relationship between the M_{TP} values obtained in Case 1 and the TL (solid line) obtained by Kim *et al*. (2012). It can be seen that the simulated M_{TP} values are close to the values of TL obtained by Kim *et al*. (2012).

On the other hand, in this study, to easily and accurately determine the opening size based on the TL, the TL was fitted by the multi-sigmoidal Gompertz function, and the fitting equation is as follows:

$$M_{TP} = 0.609 + 1.197 \times \exp\left[-\exp\{(0.195 - D_{50})/0.121\}\right] \quad (5)$$

where M_{TP}= the magnitude of Threshold Point; and D_{50}= the mean particle size.

It was confirmed that the fitted line (dotted line) by Eq. (5) agrees well with the TL (i.e., R^2=0.999). The M_{TP} of the TL corresponding to D_{50} = 1.25 mm then was derived as 1.81 mm by Eq. (5). The largest difference between the M_{TP} values of four samples for Case 1 and the TL is just 0.14 mm. It was found that when the mean particle size was fixed, the M_{TP} hardly changed regardless of the contents of fine and coarse particles in the sample. Thus, these results indicate that the TL is valid for setting the opening size for samples with different particle size distributions. Furthermore, it is expected that the TL can be used easily and accurately by Eq. (5) for setting the opening size between the shear boxes in the direct shear test regardless of saturation and unsaturated soils.

3.2 Verification for samples with different particle size distributions and mean particle sizes

In the simulation of Case 2, the influence of the change

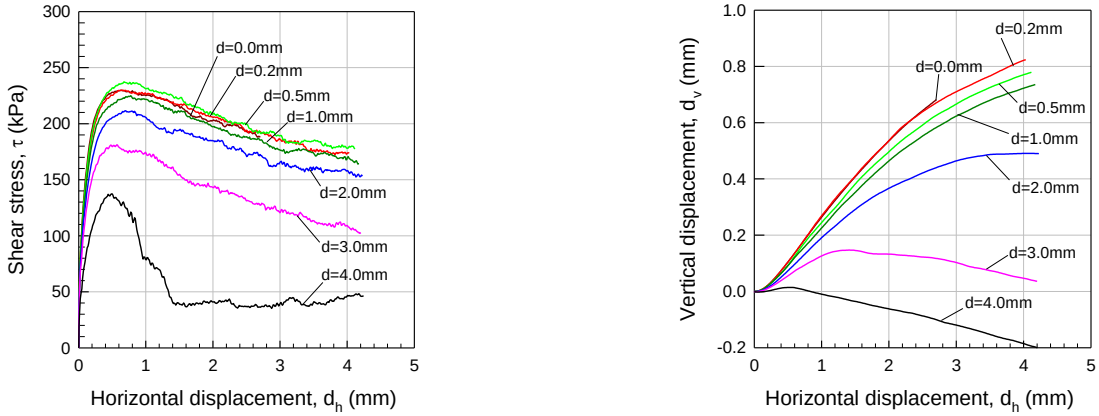

(a) d_h vs. τ (b) d_h vs. d_v

Fig. 11 Results of DEM simulation for sample A2 (slope=1.0, and particle number: 129,233)

of the mean particle size and the particle size distribution on the T.P and the TL was examined. The particle size distribution five times larger than that of Toyoura sand was defined as the standard line (sample A2) of Case 2, as shown in Fig. 9. The mean particle size was fixed as 0.89 mm and the slope of the particle size distribution was changed. As in Case 1, the particle size was limited from 0.5 to 2.0 mm. In the simulation of Case 2, to obtain different values for the mean particle size using the minimum particle size of 0.5 mm as the reference point, the grain size distribution curves of samples B2, C2, and D2 were defined as 1/1.5, 1/2, and 1/2.5 times for the slope of sample A2. The mean particle sizes for samples A2, B2, C2, and D2 were defined as 0.89, 1.08, 1.28, and 1.49 mm, respectively. The uniformity coefficients (C_u) and particle numbers are summarized in Table 5.

In the simulation of Case 2, four types of specimens with the grain size distribution curves of samples A2, B2, C2, and D2 were generated with an initial void ratio of 0.81 inside the shear box in the same way as in the previous section. The particle numbers of each sample were as follows: sample A2 (slope=1.0): 129,233; sample B2 (slope=1/1.5): 86,269; sample C2 (slope=1/2): 68,962; and sample D2 (slope=1/2.5): 56,756. In the compression process, a vertical stress of 300 kPa was applied to the specimen, and opening sizes of 0.0, 0.2, 0.5, 1.0, 2.0, 3.0, and 4.0 mm were set. Subsequently, the shearing process was conducted while maintaining a vertical stress of 300 kPa and the opening size until the maximum shear strength was confirmed.

Fig. 10(a) and 10(b) show the state of the particles for specimens of sample A2 after the shearing process for opening sizes of 0.0 and 3.0 mm, respectively. For an opening size of 3.0 mm, a large amount of particle spillage through the opening was observed during the shearing process. Fig. 11(a) and 11(b) show the relationship between the shear stress (τ) and vertical displacement (d_v) according to the horizontal displacement (d_h) of sample A2, respectively. In the relationship between horizontal displacement and shear stress, for all opening sizes, the shear stress increases rapidly at the beginning of shearing, and the maximum shear stress occurs at a horizontal displacement of around 0.5 mm. Meanwhile, in the

Table 6 Results of the internal friction angle in Case 2

Opening size, d (mm)	Internal friction angle, ϕ (degs.)			
	A2	B2	C2	D2
0.0	35.3	35.8	36.9	37.2
0.2	34.7	35.9	35.9	37.2
0.5	34.4	36.4	35.3	36.9
1.0	35.1	35.4	35.9	35.7
2.0	31.4	33.8	32.3	32.5
3.0	29.3	30.3	30.0	29.1
4.0	24.2	24.2	24.0	25.1

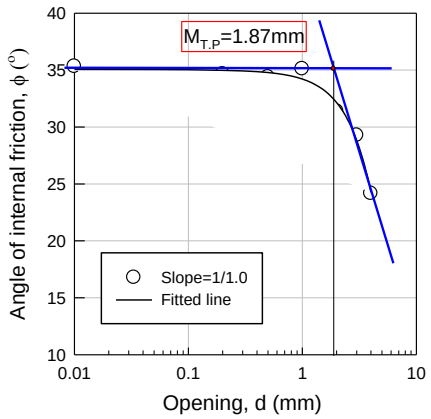

Fig. 12 Determination of the magnitude of the M_{TP} for sample A2 (slope=1.0, and particle number: 129,233)

relationship between the horizontal displacement and the vertical displacement, for all opening sizes, a dilative tendency was observed at the beginning of shearing. Then, as the shearing process progresses, it was observed that compression is dominant due to the particle outflow as the opening size increases. This tendency was most clearly observed with the initiation of shearing for an opening size of 4.0 mm. It can be stood that the shear strength was smaller because the frictional resistance between particles on the shear plane due to the particle outflow was weakened.

On the other hand, it is observed in Fig. 11 that the maximum shear stress of d= 0.5 mm is the greatest in Case

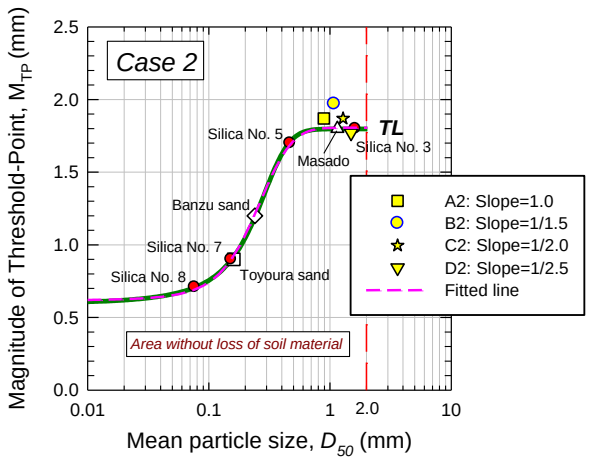

Fig. 13 Comparison of the results of the M_{TP} in Case 2 and the TL

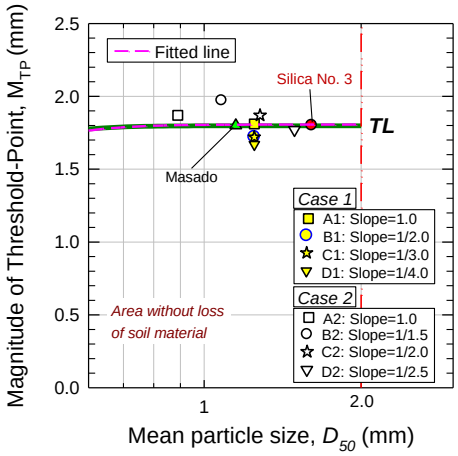

Fig. 14 Comparison of the results for Cases 1 & 2 and the TL at the extended scale for the mean particle size

2, but the dilative behavior is smaller than that of d= 0.2 mm. This can be understood that the shear strength and deformation behavior for the very small opening sizes from 0.0 mm to 0.5 mm are affected by the particle size distribution characteristics of the sample used. This tendency is also confirmed in the experimental results by Kim *et al*. (2012). In addition, compression was commonly observed in all four samples in Case 2. The results of the internal friction angles (ϕ) for all samples in Case 2 for all opening sizes are summarized in Table 6. Although the initial void ratios (i.e., dry density) of A2, B2, C2, and D2 in Case 2 are the same, the results of the obtained internal friction angle are slightly different each other in Table 6. This is due to the difference in the particle size distribution, and since the specimen of D2 contains larger particles than other samples as shown in Fig. 9, slightly larger internal friction angles were obtained. For all samples, it was found that the internal friction angle (ϕ) decreases significantly when the opening size increases beyond a certain size.

As shown in Fig. 12, the M_{TP} values for each sample in Case 2 were determined in the relationship between the internal friction angle and the opening size in the same way proposed by Kim *et al*. (2012). The results of the M_{TP} obtained for each sample are summarized in Table 5. Figure 13 shows the relationship between the results of the M_{TP} for all four samples in Case 2 and the TL (solid line) obtained by Kim *et al*. (2012). Like Case 1 above, the M_{TPs} of the TL corresponding to the mean particle sizes of four samples in Case 2 were derived as 1.80, 1.80, 1.81, and 1.81 mm by Eq. (5), respectively. Compared to the results of four samples in Case 2, the largest difference was just 0.16 mm, which was observed for the M_{TP} of sample B2 (slope=1/1.5), as shown in Table 5, and it was observed that, for all samples, the results of the M_{TP} were close to the TL values. On the other hand, Fig. 14 shows a comparison of the results for Cases 1 and 2 with the TL at the extended scale from 0.6 mm to 3.0 mm for the mean particle size. It was confirmed that the results of the M_{TP} obtained from the DEM simulation for Cases 1 and 2 were close to the values of the TL proposed from test results using real soil samples by Kim *et al*. (2012). Thus, for a mean particle diameter of 2.0 mm or less, since the change in particle size distribution has a negligible effect on the M_{TP}, it was found that the TL represents the standard value of the M_{TPs} for all samples, that is, regardless of the particle size distribution. Therefore, it can be concluded that the TL is a valid criterion to determine the appropriate opening size between the shear boxes in direct shear tests.

4. Verification of scale effect of specimens in direct shear tests

In this section, the validity of the TL for mean particle sizes smaller than 0.8 mm is examined. In general, in direct shear tests (e.g., Kim *et al*. (2012)), the shear box has a disk that is 6.0 cm in diameter and 2.0 cm in height. If the balls in the model are set with a mean soil particle size smaller than 0.8 mm for a shear box of this size, the number of balls generated exceeds 300,000; thus, there is a possibility of overloading the computation system during the DEM simulation due to the enormous number of balls. Thus, it is necessary to reduce the number of balls by adjusting the size of the shear box (i.e., specimen). To adjust the shear box size, a DEM simulation was performed to verify the scale effect of the specimen in the direct shear test. Several studies have been conducted on the scale effect in laboratory-based direct shear tests (e.g., Parsons 1936, Scarpelli and Wood 1982, Jewell and Wroth 1987, Palmeira and Milligan 1989, Stone and Muir Wood 1992, Hight and Leroueil 2003, Cerato and Lutenegger 2006). For example, Palmeira and Milligan (1989) reported that the shear box size has no significant influence of on the angles of internal friction (ϕ) when using sandy soil. However, Cerato and Lutenegger (2006) reported that the increase of the height of the shear box affects the stress distribution on the shear plane during shearing, which increases the normal stress at the top of the box and reduces it at the bottom. In this study, the scale effect of specimens in the direct shear test was verified through DEM simulation, and it was determined whether the shear box size could be adjusted.

4.1 Scale effect for shear box with a fixed D:H ratio of 3:1

First, to determine the appropriate shear box size, the

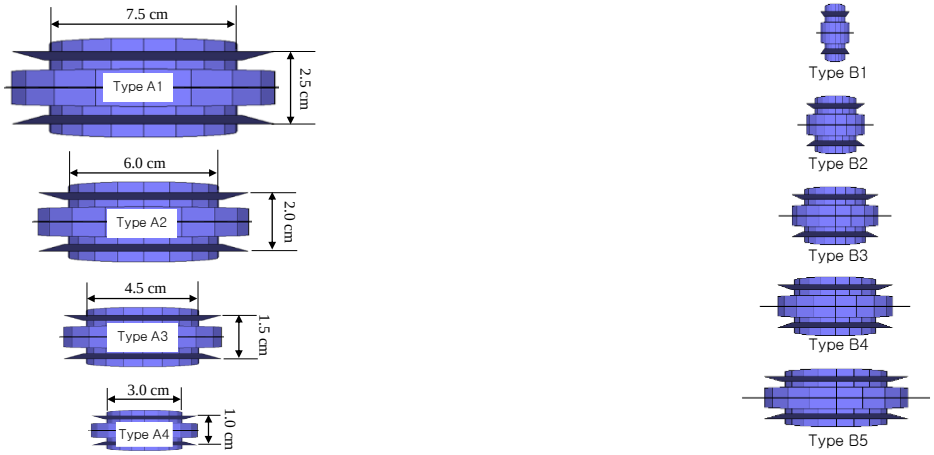

(a) Shear boxes based on the fixed ratio of *D*:*H*=3:1 (b) Shear boxes based on the varying ratiosof *D*:*H*

Fig. 15 Verification on the scale effect of the specimen of the direct shear test based on the fixed and varying ratios of D:H in DEM simulation

Table 7 Simulation conditions and results on the fixed ratio of D:H=3:1 of shear box

Type No.	Shear box size (*D*×*H*, cm)	Number of ball	Angle of internal friction, ϕ (degs.)
Type A1	7.5×2.5	90,561	39.5
Type A2	6.0×2.0	46,370	38.4
Type A3	4.5×1.5	19,564	39.1
Type A4	3.0×1.0	5,800	38.3

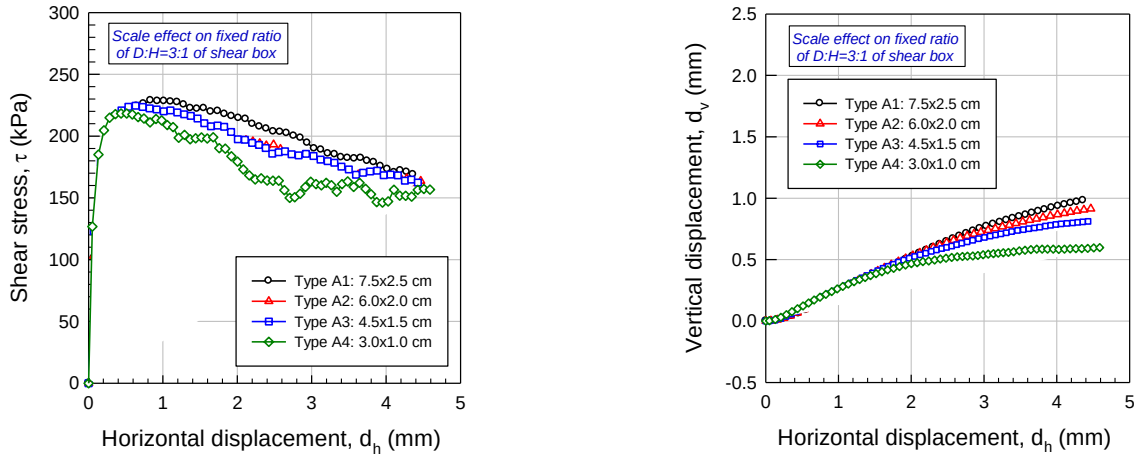

(a) d_h vs. τ (b) d_h vs. d_v

Fig. 16 Results of the DEM simulation on the fixed ratio of *D*:*H*=3:1 of shear box

Table 8 Simulation conditions and results on varying ratios of D:H of shear box

Type No.	Shear box size (*D*×*H*, cm)	Number of ball	Angle of internal friction, ϕ (degs.)
Type B1	1.0×1.2	775	63.4
Type B2	2.0×1.2	3,094	51.0
Type B3	3.0×1.2	6,958	44.8
Type B4	4.0×1.2	12,369	41.8

scale effect of the specimens for a shear box with a fixed ratio of diameter to height was examined via DEM simulation. The shear box used in this DEM simulation was 6.0 cm in diameter and 2.0 cm in height, and its ratio of diameter (*D*) to height (*H*) was 3:1. The following shear box sizes using this ratio were applied: Type A1: 7.5 × 2.5 cm; Type A2: 6.0 × 2.0 cm; Type A3: 4.5 × 1.5 cm; and Type A4: 3.0 × 1.0 cm (see Fig. 15(a)). A particle size

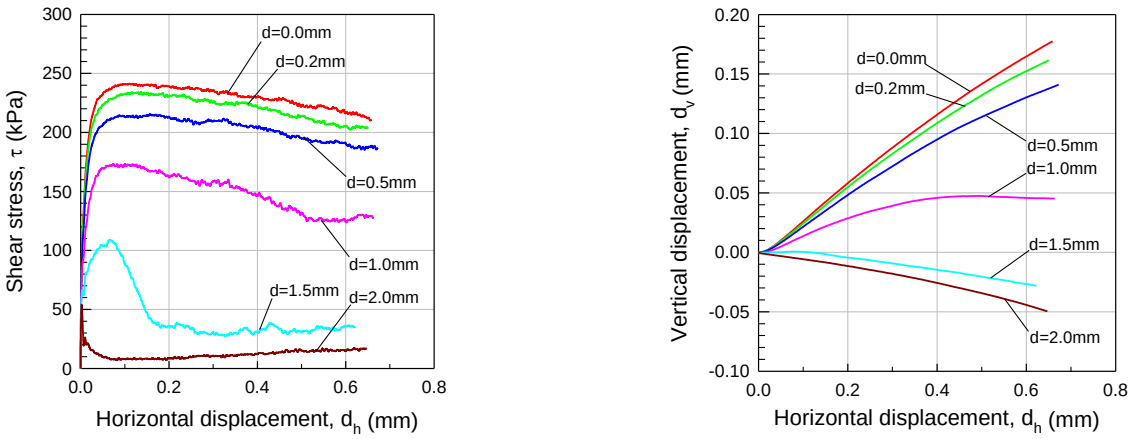

(a) d_h vs. τ (b) d_h vs. d_v

Fig. 17 Results of the DEM simulation for the opening size in Case 3-3 (D_{50}=0.242 mm)

distribution seven times larger than that of Toyoura sand was applied. The largest shear box (Type A1) has 90,561 balls, while the smallest (Type A4) has 5800 balls. The simulation conditions are summarized in Table 7. In this DEM simulation, the compression (consolidation) and shearing processes were conducted under the same conditions as the previous simulations. An opening size of 0.2 mm between the shear boxes was set before the shearing process for all cases.

Fig. 16(a) and 16(b) show the simulated relationships between the horizontal displacement, shear stress, and vertical displacement for shear boxes with a fixed *D*:*H* ratio of 3:1. All of the samples showed similar behaviors in terms of the shear strength, although there was a slight difference in the vertical displacement (i.e., dilatancy) for horizontal displacements of greater than about 2 mm. From these results, the obtained internal friction angles (ϕ) were in the range of 38° to 39°, as shown in Table 7. It was found that the shear strengths were similar to each other regardless of the shear box size. Thus, it can be concluded that the scale effect of the specimens could be neglected in the direct shear test for a *D*:*H* ratio of 3:1 in the DEM simulation.

4.2 Scale effect for shear boxes with various D:H ratios

In this section, the scale effect of the specimens was examined for shear boxes with various *D:H* ratios. In this simulation, the height of the shear box was fixed at 1.2 cm and the diameter (*D*) was changed from 1.0 to 5.0 cm. The shear box sizes were as follows: Type B1: 1.0 × 1.2 cm; Type B2: 2.0 × 1.2 cm; Type B3: 3.0 × 1.2 cm; Type B4: 4.0 × 1.2 cm; and Type B5: 5.0 × 1.2 cm (see Fig. 15(b)). A particle size distribution seven times larger than that of Toyoura sand was applied. The smallest shear box (Type B1) has 775 balls, while the largest (Type B5) has 19,321 balls. The simulation conditions for the various *D*:*H* ratios of the shear box are summarized in Table 8. The compression (consolidation) and shearing processes of the specimen were conducted under the same conditions as the previous simulations. An opening size of 0.2 mm between the shear boxes was set for all cases. The internal friction angles (ϕ) obtained from these simulations ranged from 31.4° to 63.4°, as shown in Table 8. It was found that the shear strengths for the various shear box sizes were very different from each other. Thus, it can be concluded that there is a significant scale effect of the specimens for different *D*:*H* ratios of the shear box in the DEM simulation. Finally, to reduce the number of balls by adjusting the size of the shear box, it was confirmed that a *D:H* ratio of 3:1 of the shear box should be applied.

5. Verification of the TL for D50 smaller than 0.8 mm

This section focuses on the verification of the use of the TL as a criterion for determining the appropriate opening size for the samples with a mean particle size smaller than

Table 9 Simulation conditions by adjusting the size of the shear box and the results of the M_{TP} for Case 3

No.	Shear box size (*D*×*H*, cm)	Particle size D_{50} (mm)		Number of Ball	M_{TP} (mm)
3-1	3.0×1.0	3.0 times	0.483	74,790	1.69
3-2	2.4×0.8	2.0 times	0.322	129,233	1.38
3-3	1.8×0.6	1.5 times	0.242	129,233	1.13
3-4	1.5×0.5	1.0 times	0.161	252,405	0.83

Table 10 Results of the internal friction angles according to the opening size for Case 3

Opening size, *d* (mm)	Internal friction angle, ϕ (degs.)			
	Case 3-1	Case 3-2	Case 3-3	Case 3-4
0.0	34.6	33.6	34.7	34.9
0.2	34.3	34.2	34.2	34.3
0.5	33.4	33.1	32.5	31.8
1.0	31.5	31.4	28.1	26.2
1.25	-	-	-	20.9
1.5	-	-	19.8	16.5
2.0	25.4	18.6	10.4	-
3.0	7.0	11.5	-	-
4.0	5.8	-	-	-

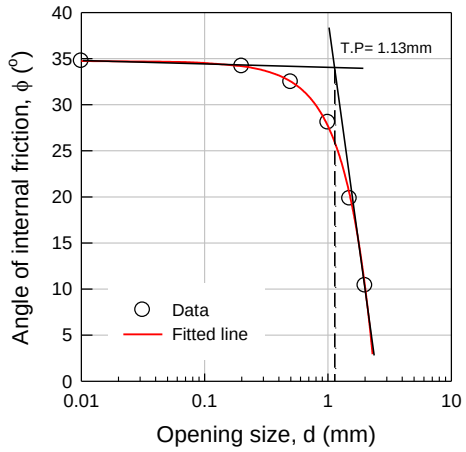

Fig. 18 Determination of the magnitude of Threshold-Point (TP) for Case 3-3

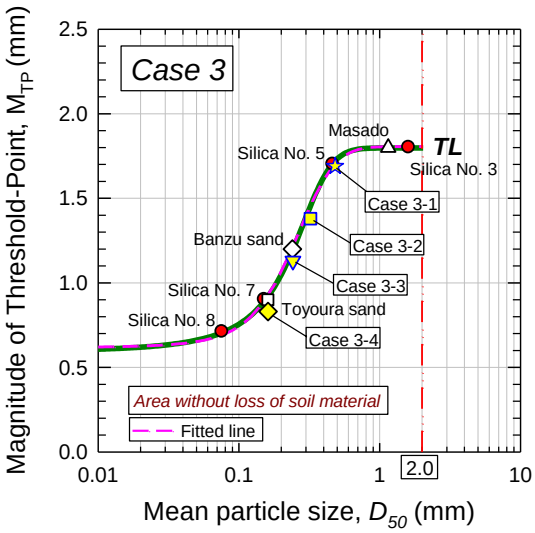

Fig. 19 Comparison of the results of the MTP for Case 3 and the TL

0.8 mm using DEM 3D simulation. Based on the optimal D:H ratio of 3:1 determined in the previous section, fourshear box sizes with a *D:H* ratio of 3:1 for Case 3 were defined as follows: Case 3-1: 3.0 × 1.0 cm; Case 3-2: 2.4 × 0.8 cm; Case 3-3: 1.8 × 0.6 cm; and Case 3-4: 1.5 × 0.5 cm. To verify the TL for a mean particle size smaller than 0.8 mm, the particle size distributions of the four cases were set as 3.0, 2.0, 1.5, and 1.0 times larger than the particle size distribution of Toyoura sand, respectively; that is, the mean particle sizes of Cases 3-1, 3-2, 3-3, and 3-4 were set as 0.483, 0.322, 0.242, and 0.161 mm, respectively. The numbers of balls for each case were as follows: Case 3-1: 74,790; Cases 3-2 and 3-3: 129,233; and Case 3-4: 252,405. Although the shear box size of Case 3-4 is very small, since the particle size distribution in this case is the same as that of Toyoura sand, it can be confirmed that the number of balls has increased significantly to about 250,000. The simulation conditions when adjusting the size of the shear box for a mean particle size smaller than 0.8 mm are summarized in Table 9. The compression (consolidation) and shearing processes of the specimen in this DEM simulation were conducted under the same conditions as the previous simulations. The opening sizes from 0.0 to 4.0 mm for Cases 3-1 and 3-2 were applied before the shearing process, while the opening sizes of 1.25 and 1.5 mm in only Cases 3-3 and 3-4 were set considering the smaller shear box sizes (i.e., Case 3-3: 1.8 × 0.6 cm; and Case 3-4: 1.5 × 0.5 cm).

Fig. 17(a) and 17(b) show the relationships between the horizontal displacement, shear stress, and vertical displacement in the DEM 3D simulations for the opening size in Case 3-3 (D_{50}=0.242 mm). As in the previous results, it was confirmed that, as the opening size increases, the shear strength and dilatancy decreases due to the outflow from the opening between the shear boxes. The results for opening sizes ranging from 0.0 to 1.0 mm showed a dilative behavior, while those for opening sizes larger than 1.0 mm eventually showed contractive behavior. The peak shear strengths were observed at a horizontal displacement of about 0.1 mm, and the results of the other two cases were similar to this tendency. It was found that the angles of internal friction (ϕ) for all cases decreased in the range from about 34.9° to 5.8° as the opening size increased from 0.0 to 4.0 mm, as summarized in Table 10.

The M_{TP}s for each case were determined as explained in Fig. 1. Fig. 18 shows the process to determine the M_{TP} for Case 3-3 using each internal friction angle. Each M_{TP} was determined based on the fitted line, and the results were as follows: Case 3-1: 1.69 mm; Case 3-2: 1.38 mm; Case 3-3: 1.13 mm; and Case 3-4: 0.83 mm. It was found that the results of the M_{TP} for three cases agreed well with the TL proposed by Kim *et al.* (2012), as shown in Fig. 19. The M_{TP}s of the TL corresponding to the mean particle sizes of four samples for Case 3 were derived as 1.69, 1.38, 1.13, and 0.83 mm by Eq. (5), respectively. Compared to the results of four samples in Case 3, the maximum difference was just 0.10 mm (Case 3-3). Therefore, it can be said that the validity and accuracy of the TL for determining the appropriate opening size for the samples with a mean particle size smaller than 0.8 mm were verified based on the these results.

6. Conclusions

In this study, the validity of the Threshold Line (TL) as a guideline for setting the opening size (*d*) between shear boxes in the experimental tests of Kim *et al.* (2012) was examined using DEM 3D simulations. This study was divided into four parts according to the variation of mean particle size and particle size distribution, scale effect, and the mean particle sizes smaller than 0.8 mm. The samples used in the DEM 3D simulations were generated based on the grain size distribution of Toyoura sand. The validity of the TL for determining the appropriate opening size was verified through a comparison between the M_{TP}s of the TL and the results obtained from the DEM 3D simulations for each case. Based on the results, the following summaries and conclusions can be drawn:

(1) In the DEM 3D simulation, the outflow of particles from the opening between the shear boxes was similar to

that observed in an experimental direct shear test of Toyoura sand by Kim *et al*. (2012). Compared to the experimental results of Kim *et al*. (2012), the shear behaviors of the direct shear test in the DEM 3D simulations were very similar in terms of the shear strength and dilatancy with the variation of the opening size during the shearing process. Thus, the reproducibility of the DEM 3D simulation of the direct shear test was confirmed, and it can be concluded that the effects on the opening size between shear boxes in the direct shear test can be investigated using the DEM 3D simulation.

(2) To examine the effectiveness of the TL for the variation of the contents of fine and coarse particles, the DEM 3D simulations were performed using four samples with a fixed mean grain size of 1.25 mm, namely samples A1, B1, C1, and D1 in Case 1. The slopes of the grain size distributions of these four samples were set to 1.0, 1/2, 1/3, and 1/4 times that of Toyoura sand, respectively. By changing the grain size distributions, the contents of fine and coarse particles of each sample were changed. From the results of the DEM 3D simulations, the magnitudes of the M_{TP} for samples A1, B1, C1, and D1 were found to be 1.81, 1.72, 1.72, and 1.77 mm, respectively. By comparing the M_{TPs} of the TL with the results for the four samples, it was shown that the largest difference between the two results was just 0.14 mm. Thus, it was found that the M_{TPs} of the samples with the same mean particle size changes very little, regardless of the content of fine and coarse particles of the samples.

(3) To examine the validity of the TL for the variation of the mean particle size and the grain size distribution, the DEM 3D simulations were performed using four samples with different mean grain sizes, namely A2, B2, C2, and D2 in Case 2. To change the mean particle sizes, the slopes of the grain size distributions of these four samples were set to 1.0, 1/1.5, 1/2, and 1/2.5 times that of Toyoura sand, respectively, and a minimum particle size of 0.5 mm was applied; the mean particle sizes of the four samples were thus defined as 0.89, 1.08, 1.28, and 1.49 mm, respectively. By comparing the M_{TPs} of the TL and the results for the four samples, the largest difference was shown to be just 0.16 mm. Thus, it was found that the TL is valid for the samples with different mean particle size and the grain size distribution.

(4) For the DEM simulation for a mean particle size smaller than 0.8 mm, it was necessary to reduce the number of balls by adjusting the size of the shear box to maximize the computational processing capability. The scale effect of the specimens was examined for fixed and varying *D*:*H* ratios of the shear box. For a fixed *D:H* ratio of 3:1, the internal friction angles (ϕ) obtained from the DEM 3D simulations using the four types of boxes ranged from 38° to 39°. Thus, it can be concluded that there is no significant scale effect of the specimens in the direct shear test for a fixed *D:H* ratio of 3:1 in the DEM 3D simulation. Meanwhile, when the *D*:*H* ratios were varied, the internal friction angles (ϕ) obtained from the DEM 3D simulations using the four types of boxes ranged from 31.4° to 63.4°. Thus, it can be concluded that there is a significant scale effect for the specimens in the direct shear test for varying *D*:*H* ratios of the shear box in the DEM 3D simulation.

(5) To verify the validity of the TL for a mean particle size smaller than 0.8 mm, the following shear box sizes with a *D:H* ratio of 3:1 were defined: Case 3-1: 3.0 × 1.0 cm; Case 3-2: 2.4 × 0.8 cm; Case 3-3: 1.8 × 0.6 cm; and Case 3-4: 1.5 × 0.5 cm. The particle size distributions of each case were set as 3.0, 2.0, 1.5, and 1.0 times that of Toyoura sand, respectively, and the mean particle sizes of each case were set as 0.483, 0.322, 0.242, and 0.161 mm, respectively. From the results of the DEM simulations, the magnitudes of the TPs for each sample were as follows: Case 3-1: 1.69 mm; Case 3-2: 1.38 mm; Case 3-3: 1.13 mm; and Case 3-4: 0.83 mm. It was found that the results of the M_{TPs} for Case 3 agreed well with those of the TL, with a maximum difference of just 0.10 mm (Case 3-3). Thus, the validity of the TL for determining the appropriate opening size for the samples with a mean particle size smaller than 0.8 mm was verified by the DEM 3D simulations. Furthermore, it can be said that the TL can be used easily and accurately by the relational equation (i.e., Eq. (5)) for setting the opening size between the shear boxes in direct shear tests regardless of saturated and unsaturated soils. It should be noted that since soil samples of 2.0 cm or less in this study were investigated, the TL can be applied to all types of soil with a particle diameter of 2.0 cm or less.

References

ASTM International (2009), *Annual Book of Standards*. Vol. 04.08, Soil and Rock, ASTM International, West Conshohocken, Pennsylvania, U.S.A.

Bian, X., Li, W., Qian, Y. and Tutumluer, E. (2019), "Micromechanical particle interactions in railway ballast through DEM simulations of direct shear tests", *Int. J. Geomech*., **19**(5), 04019031. https://doi.org/10.1061/(ASCE)GM.1943-5622.0001403.

Cerato, A.B. and Lutenegger, A.J. (2006), "Specimen size and scale effects of direct shear box tests of sands", *Geotech. Test. J.*, **29**(6), 1-10. https://doi.org/10.1520/GTJ100312.

Cho, S.E. (2008), "Infiltration analysis to evaluate the surficial stability of two-layered slopes considering rainfall characteristics", *Eng. Geol*., **105**(1), 32-43. https://doi.org/10.1016/j.enggeo.2008.12.007.

Cundall, P.A. (1971), "A computer model for simulating progressive, large-scale movement in blocky rock system", *Proceedings of the International Symposium on Rock Mechanics*, Nancy, France,

Cundall, P.A. and Strack, O.D.L. (1979), "A discrete numerical model for granular assemblies", *Geotechnique*, **29**(1), 47-65. https://doi.org/10.1680/geot.1979.29.1.47.

Gan, J.K.M., Fredlund, D.G. and Rahardjo, H. (1988), "Determination of the shear strength parameters of an unsaturated soil using the direct shear test", *Can. Geotech. J*., **25**(8), 500-510. https://doi.org/10.1139/t88-055.

Guo, P. (2008), "Modified direct shear test for anisotropic strength of sand", *J. Geotech. Geoenviron. Eng.*, **134**(9), 1311-1318. https://doi.org/10.1061/(ASCE)1090-0241(2008)134:9(1311).

Hight, D.W. and Leroueil, S. (2003), "Characterisation of soils of engineering purposes", *Proceedings of the International Workshop*, Singapore, December.

Itasca Consulting Group Inc. (2005), *PFC-3D User's Guide Version 3.1*, Itasca Consulting Group, Minnesota, U.S.A.

Jewell, R.A. and Wroth, C.P. (1987), "Direct shear test on

reinforced sand", *Geotechnique*, **37**(1), 53-68. https://doi.org/10.1680/geot.1987.37.1.53.
Kim, B.S., Shibuya, S., Park, S.W., and Kato, S. (2010), "Application of suction stress for estimating unsaturated shear strength of soils using direct shear testing under low confining pressure", *Can. Geotech. J.*, **47**(9), 955-970. https://doi.org/10.1139/T10-007.
Kim B.S., Shibuya S., Park S.W. and Kato S. (2012), "Effect of opening on shear behavior of granular material in direct shear test", *KSCE J. Civ. Eng.*, **16**(7), 1132-1142. https://doi.org/10.1007/s12205-012-1518-4.
Kim, B.S., Shibuya, S., Park, S.W. and Kato, S. (2013), "Suction stress and its application on unsaturated direct shear test under constant volume condition", *Eng. Geol.*, **155**, 10-18. https://doi.org/10.1016/j.enggeo.2012.12.020.
Kim, B.S., Park, S.W. and Kato, S. (2014), "DEM simulation on deformation mode and stress state for specimen shape in direct shear test", *Int. J. Comput. Meth.*, **11**(2), 1342004-1~18. https://doi.org/10.1142/S0219876213420048.
Kodicherla, S.P.K., Gong, G., Yang, Z.X., Krabbenhoft, K., Fan, L., Moy, C.K. and Wilkinson, S. (2019), "The influence of particle elongations on direct shear behaviour of granular materials using DEM", *Granul. Matter*, **21**(4), 1-12. https://doi.org/10.1007/s10035-019-0947-x.
Lee, S., Chang, I., Chung, M.K., Kim, Y. and Kee, J. (2017), "Geotechnical shear behavior of xanthan gum biopolymer treated sand from direct shear testing", *Geomech. Eng.*, **12**(5), 831-847. https://doi.org/10.12989/gae.2017.12.5.831.
Lin, H.D., Wang, C.C. and Wang, X.H. (2018), "A simplified method to estimate the total cohesion of unsaturated soil using an UC test", *Geomech. Eng.*, **16**(6), 599-608. https://doi.org/10.12989/gae.2018.16.6.599.
Liu, S.H. (2006), "Simulating a direct shear box test by DEM", *Can. Geotech. J.*, **43**(2), 155-168. https://doi.org/10.1139/t05-097.
Ng, C.W.W.,and Shi, Q. (1998), "A numerical investigation of the stability of unsaturated soil slopes subjected to transient seepage", *Comput. Geotech.*, **22**(1), 1-28. https://doi.org/10.1016/S0266-352X(97)00036-0.
Ni, Q., Powrie, W., Zhang, X. and Harkness, R. (2000), "Effect of particle properties on soil behavior: 3-D numerical modeling of shearbox tests", In *Numer. Methods in Geotech. Eng.* (eds G.M. Filz and D.V. Griffiths), ASCE Geotechnical Special Publication (96), 58-70. https://doi.org/10.1061/40502(284)5.
Meguid, M.A. and Khan, M.I. (2019). "On the role of geofoam density on the interface shear behavior of composite geosystems", *Int. J. Geo-Eng.*, **10**(1), 1-18. https://doi.org/10.1186/s40703-019-0103-9.
Oda, M. and Iwashita, K. (2000), "Study on couple stress and shear band development in granular media based on numerical simulation analyses", *Int. J. Eng. Sci.*, **38**(15), 1713-1740. https://doi.org/10.1016/S0020-7225(99)00132-9.
Oh, W.T. and Vanapalli, S. (2018), "Undrained shear strength of unsaturated soils under zero or low confining pressures in the vadose zone", *Vadose Zone J.*, **17**, 180024. https://doi.org/10.2136/vzj2018.01.0024.
Palmeira, E.M. and Milligan, G.W.E. (1989), "Scale effects in direct shear tests on sand", *Proceedings of 12th International Conference on Soil Mechanics and Foundation Engineering*, Rio de Janeiro, Brasil.
Parsons, J.D. (1936), "Progress report on an investigation of the shearing resistance of cohesionless soils", *Proceedings of* 1st *International Conference on Soil Mechanics and Foundation Engineering*, Cambridge, Massachusetts, U.S.A.
Scarpelli, G. and Wood, D.M. (1982), "Experimental observations of shear band patterns in direct shear", *Proceedings of the IUTAM Conference on Deformation and Failure of Granular Materials*, Delft, 472-484.
Shibuya, S., Mitachi, T. and Tamate, S. (1997), "Interpretation of direct shear box testing of sands as quasi-simple shear", *Geotechnique*, **47**(4), 769-790. https://doi.org/10.1680/geot.1997.47.4.769.
Stone, K.J.L. and Muir Wood, D. (1992), "Effects of dilatancy and particle size observed in model tests on sand", *Soils Found.*, **32**(4), 43-57. https://doi.org/10.3208/sandf1972.32.4_43.
Suhr, B., Marschnig, S., and Six, K. (2018), "Comparison of two different types of railway ballast in compression and direct shear tests: experimental results and DEM model validation", *Granular Matter*, **20**(4), 1-13. https://doi.org/10.1007/s10035-018-0843-9.
Sweta, K., and Hussaini, S.K.K. (2018), "Effect of shearing rate on the behavior of geogrid-reinforced railroad ballast under direct shear conditions", *Geotext. Geomembranes*, **46**(3), 251-256. https://doi.org/10.1016/j.geotexmem.2017.12.001.
Tatsuoka, F., Nakaumura, S., Huang, C.C. and Tani, K. (1990), "Strength anisotropy and shear band direction in plane strain tests in sand", *Soils Found.*, **30**(1), 35-54. https://doi.org/10.3208/sandf1972.30.35.
Thornton, C. (2000), "Numerical simulations of deviatoric shear deformation of granular media", *Geotechnique*, **50**(1), 43-53. https://doi.org/10.1680/geot.2000.50.1.43.
Vanapalli, S.K., Fredlund, D.G., Pufahl, M.D., and Clifton, A.W. (1996), "Model for prediction of shear strength with respect to soil suction", *Can. Geotech. J.*, **33**(3), 379-392. https://doi.org/10.1139/t96-060.
Wang, G. and Sassa, K. (2003), "Pore-pressure generation and movement of rainfall-induced landslides: Effects of grain size and fine-particle content", *Eng. Geol.*, **69**(1-2), 109-125. https://doi.org/10.1016/S0013-7952(02)00268-5.
Xu, W.J., Li, C.Q. and Zhang, H.Y. (2015), "DEM analyses of the mechanical behavior of soil and soil-rock mixture via the 3D direct shear test", *Geomech. Eng.*, **9**(6), 815-827. http://doi.org/10.12989/gae.2015.9.6.815.
Yan, W.M. (2009), "Fabric evolution in a numerical direct shear test," *Comput. Geotech.*, **36**(4), 597-603. https://doi.org/10.1016/j.compgeo.2008.09.007.
Yatabe, R., Oshima, A., and Suzuki, K. (1995), "Results of round robin test on direct shear test", *Proceedings of International Symposium on Direct Shear Box Testing of Soils*, Paris, France, September.
Zhang, L. and Thornton, C. (2007), "A numerical examination of the direct shear test", *Geotechnique*, **57**(5), 343-354. https://doi.org/10.1680/geot.2007.57.4.343.

GC